

Properties of metal-insulator transition and electron spin relaxation in GaN:Si

A. Wolos

Institute of Physics, Polish Academy of Sciences, Al. Lotnikow 32/46, 02-668 Warsaw, Poland

Z. Wilamowski

Institute of Physics Polish Academy of Sciences, Al. Lotnikow 32/46, 02-668 Warsaw, Poland and Faculty of Mathematics and Computer Sciences, University of Warmia and Mazury, ul. Zolnierska 14, 10-561 Olsztyn, Poland

M. Piersa and W. Strupinski

Institute of Electronic Materials Technology, ul. Wolczynska 133, 01-919 Warsaw, Poland

B. Lucznik, I. Grzegory, and S. Porowski

Institute of High Pressure Physics of the Polish Academy of Sciences, Unipress, ul. Sokolowska 29/37, 01-142 Warsaw, Poland

(Received 9 July 2010; revised manuscript received 2 December 2010; published 25 April 2011)

We investigate the properties of doping-induced metal-insulator transition in GaN:Si by means of electron spin resonance and the Hall effect. While increasing the doping concentration, Si-related bands are formed below the bottom of the GaN conduction band. The D^0 band of single-occupied Si donor sites is centered 27 meV below the bottom of the GaN conduction band, and the D^- band of double-occupied Si states is centered at 2.7 meV below the bottom of the GaN conduction band. Strong damping of the magnetic moment occurs due to filling of the D^- states at Si concentrations approaching the metal-insulator transition. Simultaneously, shortening of electron spin relaxation time due to limited electron lifetime in the single-occupied D^0 band is observed. The metal-insulator transition occurs at the critical concentration of uncompensated donors equal to about $1.6 \times 10^{18} \text{ cm}^{-3}$. Electronic states in metallic samples beyond the metal-insulator transition demonstrate the nonmagnetic character of double-occupied states.

DOI: [10.1103/PhysRevB.83.165206](https://doi.org/10.1103/PhysRevB.83.165206)

PACS number(s): 71.30.+h, 72.20.Ee, 76.30.Da

I. INTRODUCTION

Gallium nitride is a wide-band-gap semiconductor finding application in blue and UV optoelectronics¹ and high-power electronics.² It is also being investigated for use in spintronics^{3,4} due to its weak spin-orbit interaction and expected long electron spin coherence. There is also considerable interest in doping GaN with transition metals in order to combine magnetic and semiconducting properties, likewise for use in spintronic devices.⁵ Silicon as a popular shallow donor in GaN serves as a source of effective-mass electrons, allowing us to obtain n -type material. As both electron transport and spin coherence in n -type semiconductors are practically determined by the properties of donor bands, we present systematic studies of the Si doping-induced bands in GaN. The investigations were performed by means of electron spin resonance (ESR) and the Hall effect. In particular, we focus on properties of GaN:Si being close to the metal-insulator transition (MIT).

The critical Si concentration for the MIT in GaN has already been theoretically estimated,^{6,7} however the exact nature of the transition has not been investigated experimentally. In this paper, we present a classical analysis of electron transport close to the MIT, evaluating activation energies of the resistivity and the Hall concentration. Their dependence on the doping allows us to determine the critical concentration for the MIT. The electron transport data are analyzed within Shklovskii's formalism,⁸ which distinguishes the following three activation energies: E_1 , to the GaN conduction band; E_2 , the activation energy to double-occupied donor states; and E_3 , the hopping activation energy. Such analysis is presented in Sec. V.

ESR provides a deeper understanding of the nature of the MIT in GaN:Si. The measurements show unambiguously that the electronic magnetic moment is damped when approaching the critical concentration for the MIT, which is consistent with filling nonmagnetic double-occupied donor states (D^-). Simultaneously, the electron lifetime in the single-occupied donor band (D^0) becomes shortened due to excitations to the D^- band. In metallic samples being well beyond the MIT, all the conducting electrons occupy nonmagnetic electronic states.

II. SAMPLES AND EXPERIMENTAL DETAILS

Two sets of GaN:Si crystals were studied. Epilayers were grown by metal-organic chemical vapor deposition (MOCVD) on a sapphire substrate, with donor concentration varying between 10^{17} and 10^{19} cm^{-3} . Epilayers were thinner than $2 \mu\text{m}$. Bulk samples were obtained by hydride vapor phase epitaxy (HVPE) on high-pressure-grown platelike GaN seeds. Details of the growth procedure are summarized in Ref. 9. The thickness of the HVPE samples ranged up to 1 mm, while lateral dimensions were typically $4 \times 4 \text{ mm}^2$. Dislocation density ranged up to 10^7 cm^{-3} .¹⁰ Si concentration varied between 10^{17} and 10^{19} cm^{-3} . The large volume of the HVPE crystals allowed us to perform precise ESR measurements.

ESR measurements were performed using a Bruker ESP 300 spectrometer operating in X-band with a microwave frequency of 9.5 GHz. Temperature was varied down to 2.5 K using an Oxford continuous-flow cryostat. Magnetic field was calibrated with a DPPH marker.

III. ELECTRON SPIN RESONANCE OF EFFECTIVE-MASS DONORS IN GaN

ESR of residual donors in wurtzite GaN films grown by MOCVD has been studied by Carlos and co-workers.¹¹ The anisotropic g factor of effective-mass donors (D^0) has been determined to be equal to $g_{\parallel} = 1.951$ and $g_{\perp} = 1.948$, while the mean g value has been explained using the five-band $\mathbf{k}\cdot\mathbf{p}$ model. Resonance lines characterized by this g factor were next reported in crystals obtained by the following different techniques: MOCVD-, MBE-, and HVPE-grown GaN doped with Si, or intentionally undoped, as well as in intentionally undoped AMMONO-GaN micropowders.^{12,13} In this work, we extended the ESR studies of GaN on highly Si-doped samples grown by HVPE to study the properties of the metal-insulator transition.

ESR spectra of Si donors in HVPE-GaN ($T = 2.5$ K) are shown in Fig. 1. The resonance recorded for a sample with the lowest silicon concentration in a series, $n_{\text{Si}} - n_a = 3.3 \times 10^{16} \text{ cm}^{-3}$ (where n_{Si} denotes total Si concentration, n_a is the concentration of compensating acceptors, and the parameters will be determined from Hall measurements in subsequent sections), has a symmetric Lorentzian line shape. For higher Si concentrations, $n_{\text{Si}} - n_a = 1.5 \times 10^{18}$ and $1.6 \times 10^{18} \text{ cm}^{-3}$, the line shape is Dysonian, characteristic of conducting samples. For a sample with the highest Si concentration, $n_{\text{Si}} - n_a = 5.3 \times 10^{18} \text{ cm}^{-3}$, we did not record any resonance.

The resonance line shapes become modified while elevating temperature, reflecting changes in GaN:Si conductivity. We performed an analysis of the ESR signals exploiting Dyson's formalism.^{14,15} This allowed us to determine skin depth δ for microwave penetration, which at $T = 2.5$ K is equal to > 100 ,

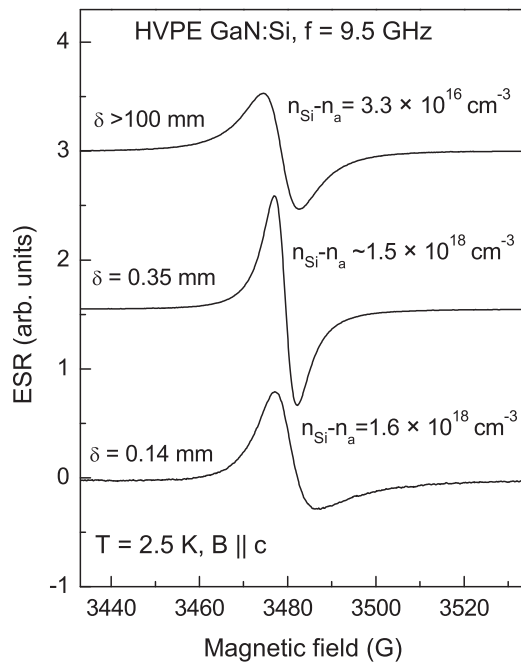


FIG. 1. ESR spectra of neutral Si donors (D^0) in HVPE-grown GaN. The signal evolves from Lorentzian line shape in isolating samples to a Dysonian line shape in conducting samples. n_{Si} denotes total Si concentration; n_a denotes concentration of acceptors. δ stays for the skin depth of microwave penetration.

0.2, and 0.14 mm for samples with $n_{\text{Si}} - n_a$ equal to 3.3×10^{16} , 1.5×10^{18} , and $1.6 \times 10^{18} \text{ cm}^{-3}$, respectively. The performed analysis will allow us to subtract contribution of the skin effect from the amplitude of the ESR signals discussed in Sec. VI.

IV. ELECTRON SPIN RELAXATION IN GaN:Si

ESR in n -type GaN has been investigated recently by time-resolved optical methods.^{3,4} The authors of Ref. 3 have observed the nonmonotonic variation of spin lifetimes with doping, with the longest low-temperature spin lifetime equal to 20 ns for intermediate doped samples. Interestingly, the measured spin coherence appeared to be robust to the presence of a large number of dislocations.

ESR provides classical methods for the determination of transverse (T_2) and longitudinal (T_1) spin relaxation times. A resonance linewidth is connected to spin relaxation through the relation $\Delta B_{\text{HWHM}} = 1/(\gamma T_2) = 1/(2\gamma T_1) + 1/(\gamma T_2')$, where γ is the electron gyromagnetic ratio and T_2' denotes a dephasing time related to all effects other than those for T_1 .

The longitudinal spin relaxation time for a sample with $n_{\text{Si}} - n_a = 3.3 \times 10^{16} \text{ cm}^{-3}$ was estimated from the ESR signal using a standard saturation method.^{16,17} Figures 2(a) and 2(b) show the dependence of the integrated amplitude and of the linewidth on microwave power. At low microwave powers, the amplitude grows like the square root of the power. When the power absorbed is comparable to the power relaxed by the system, the amplitude saturates. Saturation effects are visible also as the broadening of the resonance line [Fig. 2(b)]. The saturation method has been described in classical ESR textbooks, where one can find formulas to fit the microwave power dependence; see, e.g., Refs. 16 and 17. Fitting the power dependence of the data shown in Fig. 2, one gets T_1 equal to about 3000 ns at a temperature of 2.5 K, and 12000 ns at a temperature of 40 K. This gives the contribution to the broadening of the resonance line less than 0.01 G in both cases. The measured resonance linewidth is higher than 3 G in the whole temperature range, thus the contribution of longitudinal relaxation to the linewidth can be neglected. For samples with higher Si concentration, the amplitude of the resonance does not saturate up to the microwave power of 200 mW. This means T_1 is shorter than about 3000 ns. The contribution of T_1 to the linewidth cannot be excluded in these cases.

The dependence of the ESR linewidths on temperature for a set of HVPE-GaN:Si is shown in Fig. 3. The sample with the lowest Si concentration ($n_{\text{Si}} - n_a = 3.3 \times 10^{16} \text{ cm}^{-3}$) is very typical.¹¹ The resonance line, which is inhomogeneously broadened due to fluctuations of effective magnetic field felt by the donor electrons (e.g., originating from super-hyperfine interactions with spins of neighboring nuclei), undergoes motional narrowing while elevating temperature. The linewidth narrows from 10 G (T_2 elongates from 5.6 ns) at $T = 2.5$ K down to 2.7 G (21 ns) at $T = 30$ K. The narrowing mechanism is related to thermally activated motion of electrons leading to an averaging of effective magnetic field fluctuations, and thus to a narrowing of the resonance. Typically, activation energies of the motional narrowing are equal to the activation energies for the resistivity. This is clearly visible, e.g., on an example of ESR in n -type ZnO.¹⁸ In the case of GaN, the effect of motional narrowing must be shadowed by other relaxation mechanisms.

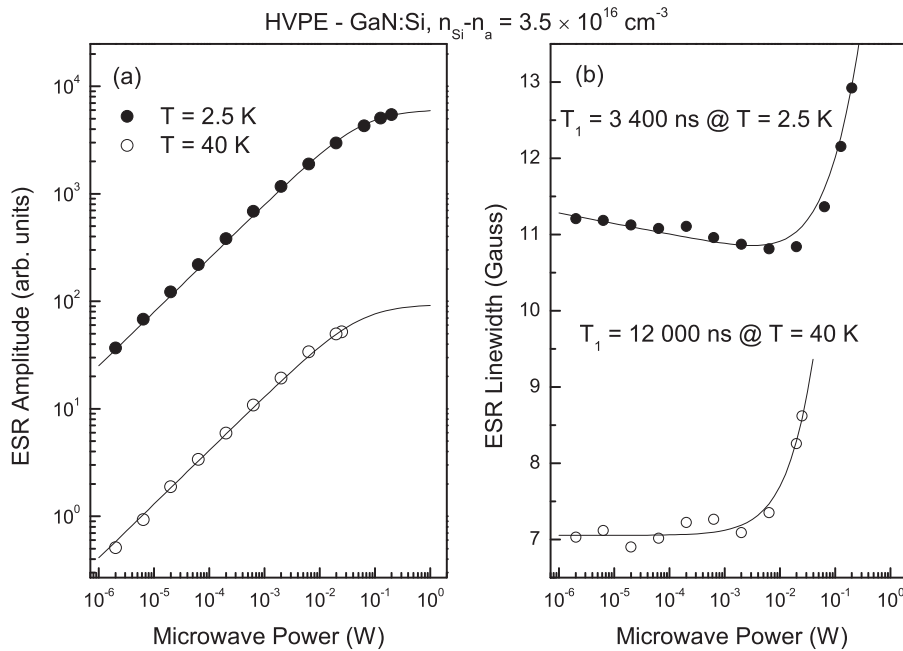


FIG. 2. Determination of the neutral donor electron spin relaxation time T_1 from a standard saturation method in a sample having $n_{\text{Si}} - n_a = 3.3 \times 10^{16} \text{ cm}^{-3}$. The dependence of the amplitude (a) and the linewidth (b) of the ESR signal on microwave power is modeled with standard formulas^{16,17} yielding T_1 equal to 3400 ns at $T = 2.5 \text{ K}$, and 12000 ns at $T = 40 \text{ K}$, respectively. The inhomogeneously broadened resonance line recorded at $T = 2.5 \text{ K}$ undergoes a slight narrowing with increasing microwave power below saturation. This effect is not visible in the homogeneous broadened line recorded at $T = 40 \text{ K}$.

The activation energy of the narrowing determined for the $n_{\text{Si}} - n_a = 3.3 \times 10^{16} \text{ cm}^{-3}$ sample (0.5 meV) is too low to be attributed solely to the motional effect. The activation energy for the resistivity is expected to be of the order of a few meV in this case (see Sec. V).

The ESR linewidth undergoes subsequent broadening with an activation energy of 11 meV while further elevating temperature. The T_2 shortens down to 4.4 ns at $T = 50 \text{ K}$. The broadening is correlated with excitation of the donor electrons

to the GaN conduction band, promoting interaction with GaN lattice (acoustic) phonons.¹¹

While increasing donor doping (reducing the distance between the donor sites), the magnitude of exchange interactions is increased. This leads to an averaging of the local magnetic field for the ensemble of exchange-coupled electrons. As a result, the inhomogeneous contribution to the linewidth is eliminated, narrowing the resonance line.¹⁹ Indeed, this effect is observed in a sample with $n_{\text{Si}} - n_a = 1.5 \times 10^{18} \text{ cm}^{-3}$, for which the low-temperature linewidth is reduced down to about 4.3 G ($T_2 = 13.6 \text{ ns}$), and no further narrowing effects are visible with varied temperature.

The two samples with higher Si doping are qualitatively different from lighter doped crystals. Besides the homogeneous character of the resonance line, a new broadening effect appears. A shortening of the ESR time T_2 is clearly visible both with increasing the Si doping and with elevating temperature. The low-temperature T_2 shortens from 13.6 ns for the $n_{\text{Si}} - n_a = 1.5 \times 10^{18} \text{ cm}^{-3}$ sample down to 6.8 ns for the $n_{\text{Si}} - n_a = 1.6 \times 10^{18} \text{ cm}^{-3}$ sample. The effect of temperature is even more pronounced, reducing the spin relaxation time to 1.7 ns at $T = 20 \text{ K}$ for the latter sample.

The ESR results are in good agreement with those obtained in Ref. 3 by time-resolved Faraday rotation, despite the fact that optical methods may be influenced by processes of carrier excitation and recombination. The longest spin relaxation times T_2 in our samples are observed either due to exchange or to motional narrowing, the mechanisms which remove the effects of inhomogeneous broadening. The resulting low-temperature spin relaxation times are of the order of 14–21 ns, similar to that reported in Ref. 3. One can attempt to assign the long spin relaxation times to the fundamental spin-orbit interactions in GaN. The interplay between (i) broadening due to super-hyperfine interaction with neighboring nuclei, (ii) exchange narrowing, and (iii) motional narrowing leads to the nonmonotonic variation of spin relaxation times with the doping. Additionally, (iv) a new mechanism becomes

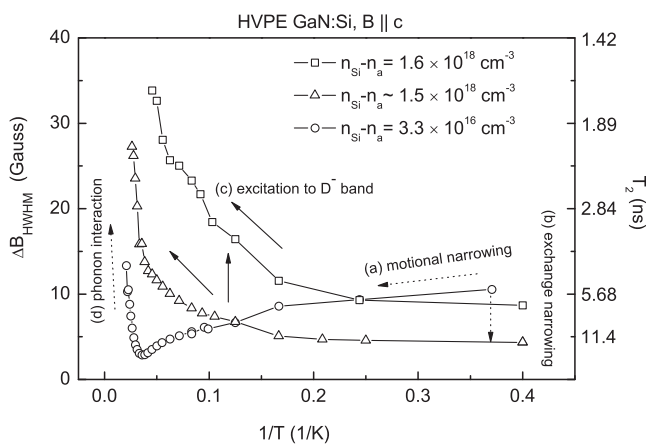


FIG. 3. Temperature dependence of the resonance linewidth (and corresponding spin relaxation time T_2 , right vertical scale) for HVPE-grown GaN:Si. Qualitative analysis of the dominating spin relaxation mechanisms is indicated with arrows: (a) hopping leads to the motional narrowing with increasing temperature in lightly doped samples, (b) exchange narrowing mechanism elongates electron spin relaxation time T_2 when increasing Si doping, (c) excitation to double-occupied donor band D^- shortens electron spin relaxation time both when increasing temperature and approaching critical concentration for the metal-insulator transition, and (d) interaction with GaN lattice phonons shortens the T_2 at high temperatures.

pronounced when approaching the metal-insulator transition. A drastic shortening of T_2 has been observed in both time-resolved Faraday rotation and in the ESR experiment. We will discuss this problem in Sec. VI.

V. HALL MEASUREMENTS

To illustrate the formation of Si donor bands in GaN, we performed Hall measurements on both HVPE-grown GaN:Si and MOCVD-grown epilayers. Symbols in Fig. 4 show Hall concentration, mobility, and the resistivity measured versus temperature. The results are very typical for impurity-related conduction in a standard semiconductor. One can describe the Hall data by a classical Shklovskii formalism based on

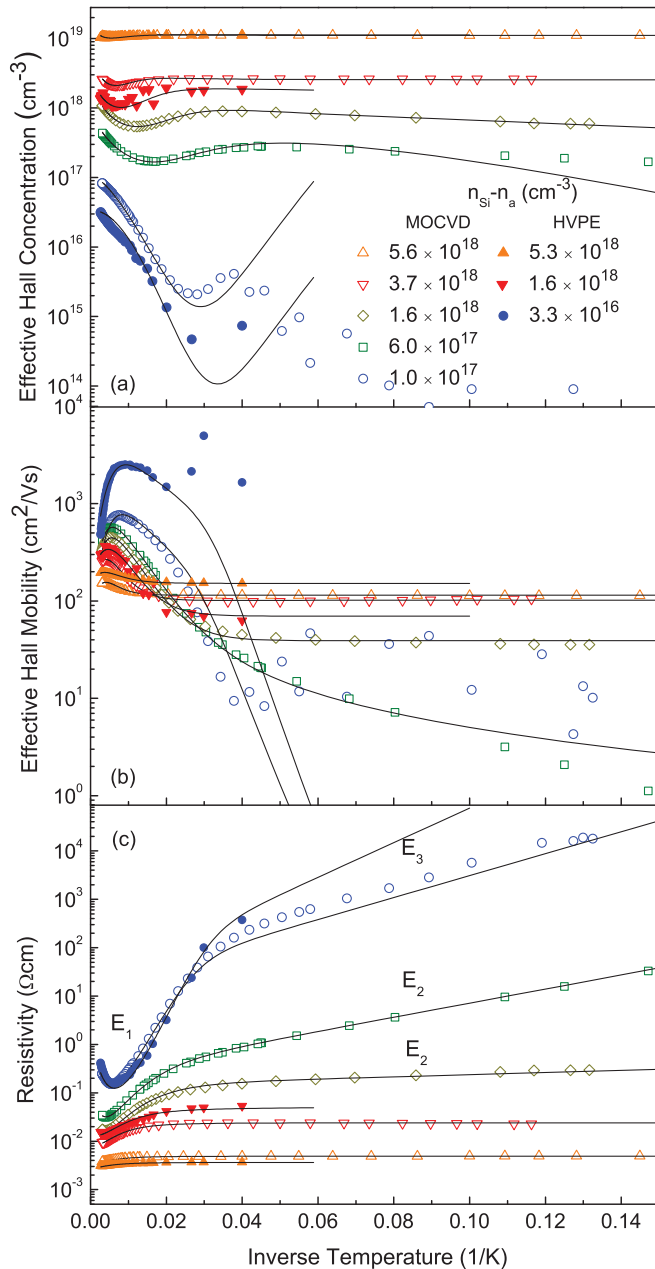


FIG. 4. (Color online) (a) Effective concentration, (b) mobility, and (c) resistivity determined by Hall measurements for a series of MOCVD- and HVPE-grown GaN:Si.

the early works of Mott and Hubbard.⁸ Solid lines in Fig. 4 are fitted according to this model, employing the same fitting procedure as was used in Ref. 20. Table I displays the obtained Hall parameters, which are as follows: concentration of uncompensated Si donors, $n_{\text{Si}} - n_a$; compensation ratio, $K = n_{\text{Si}}/n_a$; and three activation energies, E_1 , E_2 , and E_3 .

Electric conductivity is decomposed here to the three mechanisms: conduction in the host crystal conduction band activated with energy E_1 , and two mechanisms related to the conduction due to donor impurities. A hopping conduction relates to tunneling of electrons between occupied (D^0) and empty (D^+) donor sites. It is thermally activated with energy E_3 and characterized by a negligent effective Hall mobility. The third conduction mechanism distinguished here is related to the motion of electrons over singly filled neutral donor sites, with activation energy denoted by most authors by E_2 . The extra electron occupying the neutral donor site forms a D^- center. Because of a large radius of D^- centers, they overlap strongly at intermediate impurity concentration, allowing electric transport. Simultaneously, the mobility in the D^- band is considerably higher than for the hopping conduction. The D^- band of double-occupied donors has sometimes been identified with the upper Hubbard subband.^{8,21-23}

Basing on the above model, the following features of electron transport in GaN:Si are recognized. High-temperature conductivity is dominated by electron conduction in the GaN conduction band, activated with energy E_1 . The E_1 , which for compensated lightly doped samples corresponds to the ionization energy of an isolated donor, E_0 , decreases systematically while increasing Si doping due to broadening of the D^0 band. Shklovskii gives the following formula for the E_1 :⁸

$$E_1 = E_0 - f(K) \frac{e^2}{4\pi \epsilon \epsilon_0} n_{\text{donor}}^{1/3}. \quad (1)$$

TABLE I. Electric transport parameters of MOCVD- and HVPE-grown GaN:Si determined from Hall experiment: n_{Si} is the Si donor concentration; n_a is the acceptor concentration; $K = n_a/n_{\text{Si}}$ denotes the compensation ratio; E_1 , E_2 , and E_3 are the conduction-band transport activation energy, activation energy to double-occupied donor band, D^- , and hopping activation energy, respectively. An asterisk denotes a sample for which we were unable to determine transport parameters from Hall data due to parasite currents. In that case, we relied on resistivity values determined from the Dysonian line shape of the ESR signal (in particular, E_2 was determined in this way) and on the technological data.

$n_{\text{Si}} - n_a$ (cm ⁻³)	$K = n_a/n_{\text{Si}}$	E_1 (meV)	E_2 (meV)	E_3 (meV)
MOCVD-GaN:Si				
1.0×10^{17}	0.37	15.9		4.5
6.0×10^{17}	0.28	5.6	2.9	
1.6×10^{18}	0.18	3.1	0.6	
3.7×10^{18}	0.28	0	0	
5.6×10^{18}	0.26	0	0	
HVPE-GaN:Si				
3.3×10^{16}	0.30	21.5		7.1
$\sim 1.5 \times 10^{18}$ *			0.6	
1.6×10^{18}	0.27	0	0	
5.3×10^{18}	0.46	0	0	

Here, the activation energy depends on the electrostatic energy of electrons separated by a distance equal to the average distance between donor sites. Effects of compensation are taken into account by including $f(K)$, a function of the compensation parameter K . For low silicon concentration limit, the E_1 tends to $E_0 = 27$ meV in GaN, which is in good agreement with the optical Si level, 22–29 meV.^{24,25} E_1 takes value of about 21.5 meV for the HVPE sample with a Si concentration $n_{\text{Si}} - n_a = 3.3 \times 10^{16} \text{ cm}^{-3}$, and tends to zero at the critical concentration of about $n_{\text{Si}} - n_a = 1.6 \times 10^{18} \text{ cm}^{-3}$ (Fig. 5).

At low temperatures, a classical nearest-neighbor hopping is observed in lightly doped samples having $n_{\text{Si}} - n_a$ below $1.0 \times 10^{17} \text{ cm}^{-3}$. Hopping appears in Hall measurements as a rapid drop of effective mobility and a simultaneous apparent increase in Hall concentration. This occurs for the $n_{\text{Si}} - n_a = 1.0 \times 10^{17}$ sample at a temperature of about 40 K. Below this temperature, hopping conduction dominates, mobility is too low to be measured, and the effective Hall concentration returns random values. The thermal activation energy E_3 is equal to 4.5 meV for this sample. Such behavior is not observed in stronger doped samples.

In MOCVD-grown samples with $n_{\text{Si}} - n_a = 6.0 \times 10^{17}$ and $1.6 \times 10^{18} \text{ cm}^{-3}$, there is lack of the typical hopping transport at low temperatures. Instead, the conductivity shows low but definite mobility, allowing us to attribute the dominating conductivity mechanism to the E_2 -type of electron conduction. The E_2 mechanism has often been attributed to the motion of electrons over single-filled neutral donors, the conduction in

the D^- band.^{8,22} The D^- notation originates from the physics of defects in solids and denotes a negatively charged donor in a substitutional position.²¹ In the Mott-Hubbard model of the metal-insulator transition, it is considered that an extra electron can be added to the lattice of single-filled donor sites, resulting in splitting of the donor band into two subbands: a lower Hubbard subband of single-filled states and an upper Hubbard subband of double-filled states.²³ The subbands are separated by the energy U (the Hubbard U) equal to the interaction energy of two electrons of opposite spins located at the same site. It is natural to link the Mott-Hubbard picture with defect models to identify the upper Hubbard subband with the D^- band of double-occupied donors. This relation has often been pointed out in the literature.^{8,22,26} From the Hall data, one can determine the location of the D^- band in GaN:Si, which is about 2.7 meV below the bottom of the GaN conduction band (for the $n_{\text{Si}} - n_a = 6.0 \times 10^{17} \text{ cm}^{-3}$ sample). The D^0 band is placed about 27 meV below the bottom of the GaN conduction band, which gives a splitting of the two silicon donor subbands equal to about 24.3 meV, which is equal to 0.9 of the ionization energy of an isolated Si donor. This is a fairly expected value in the Mott-Hubbard description ($U = 0.96E_0$ in the original model).^{6,8}

The activation energy E_2 in GaN:Si samples decreases with increasing Si doping. It is worth noting that it tends to zero at the same critical concentration as the vanishing of the E_1 activation energy, Fig. 5. The situation when the E_1 and the E_2 tend to zero at the same critical impurity concentration is not a universal rule for III-V semiconductors. For example, it was shown earlier that in GaAs doped with an Mn acceptor, the E_2 vanishes at the critical concentration of about $3 \times 10^{19} \text{ cm}^{-3}$, above which metallic conduction occurs in the Mn acceptor band, while the E_1 tends to zero at much higher concentration equal to about $2 \times 10^{20} \text{ cm}^{-3}$.²⁰ A similar situation appears in antimony-doped germanium.²² In our case, however, we cannot distinguish unambiguously two separate critical concentrations for vanishing of the E_1 and of the E_2 , respectively. Although a slight slope in Hall concentration data is visible at high temperatures for all samples having concentration higher than $n_{\text{Si}} - n_a = 1.6 \times 10^{18} \text{ cm}^{-3}$ (higher than the MIT), we cannot attribute this slope to the nonzero E_1 activation energy. It is related rather to the temperature dependence of the density of states. In nondegenerate semiconductors, the concentration n of electrons in the conduction band can be approximately expressed as $n \sim N_c \exp(E_1/kT)$, where N_c is the effective density of states in the conduction band dependent on temperature like $T^{3/2}$. One can see that even for E_1 equal to zero, the electron concentration in the conduction band is not independent of temperature. On the other hand, for highly degenerate semiconductors, one can show that the $T^{3/2}$ dependence cancels out and n becomes a constant number.²⁷ There exists a region of donor concentrations in the vicinity of the metal-insulator transition which represents intermediate properties between a nondegenerate and a highly degenerate picture. Summarizing, it seems for us that both activation energies E_1 and E_2 vanish at the same critical concentration.

It is also worth noting that the critical concentration for the MIT depends on the compensation. We have accepted a value of $1.6 \times 10^{18} \text{ cm}^{-3}$, which is evidently an onset of metallic conduction in HVPE-grown samples. In MOCVD crystals,

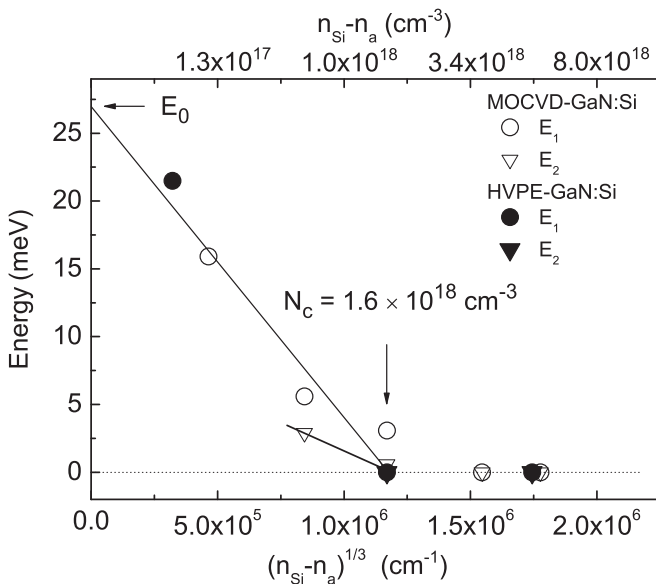


FIG. 5. Conduction-band transport activation energy, E_1 , and activation energy to double-occupied donor band, E_2 , are plotted vs reciprocal distance between uncompensated Si donors, $n_{\text{Si}} - n_a$. E_0 denotes conduction-band activation energy at the low doping limit, corresponding to the location of the isolated donor level with respect to the GaN conduction band. The critical concentration for the metal-insulator transition, corresponding to vanishing of both the activation energies, E_1 and E_2 , is equal to $N_c = 1.6 \times 10^{18} \text{ cm}^{-3}$. Solid lines: upper line is a fit of Eq. (1), where $n_{\text{Si}} - n_a$ equal to n_{donor} was assumed; lower line is a guide to the eye.

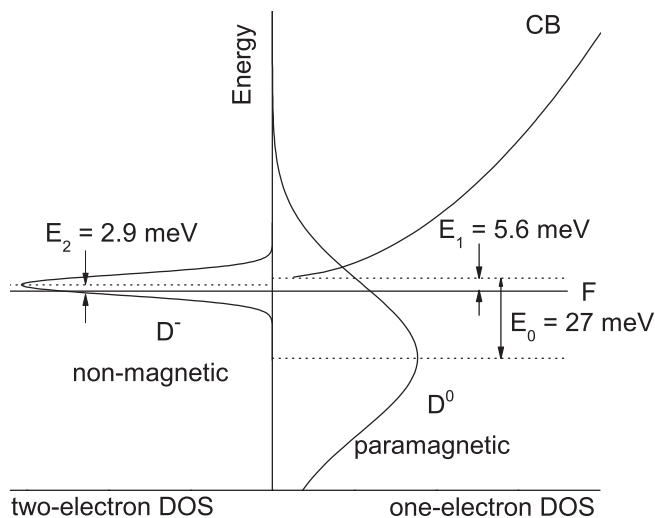


FIG. 6. Schematic diagram of the density of states (DOS) in GaN:Si with $n_{\text{Si}} - n_a = 6.0 \times 10^{17} \text{ cm}^{-3}$. One-electron DOS is shown in the right panel, including the GaN conduction band (CB) and the D^0 band of single-occupied Si donors. Left panel represents two-electron density of states with the D^- band of double-occupied donors. F denotes the Fermi level. Conduction-band activation energy, E_1 , activation energy to double-occupied donor band, E_2 , and activation energy of an isolated Si donor, E_0 , are determined from Hall experiment.

the sample with $n_{\text{Si}} - n_a = 1.6 \times 10^{18} \text{ cm}^{-3}$ still shows small thermal activation in conductivity, so the MIT occurs at a somewhat higher Si concentration. This small discrepancy may be attributed to experimental error in determination of the Si concentration, or to the dependence on the compensation. Expression of the critical concentration in terms of a number of neutral donors, $n_{\text{Si}} - n_a$, allows us to take into account compensation effects, however that may not be sufficient. It was pointed out in Ref. 22 that the effect of compensation on E_2 involves more than an increase in the average separation between neutral donors.

Figure 6 shows a schematic representation of the density of states introduced by the Si doping in GaN, shown in an example of a sample having $n_{\text{Si}} - n_a = 6.0 \times 10^{17} \text{ cm}^{-3}$. Both the D^0 band of single-occupied donor states and the D^- subband of double-occupied states are shown. To explain the definite E_2 activation energy, the D^- band is plotted as a narrow peak in the density of states, narrower than the D^0 subband. This is in contrast to the larger localization radius of the D^- states, which should lead to a larger bandwidth. We will disregard this inconsistency, as so far there is lack of a plausible explanation (see the discussion in Ref. 8).

The critical Si concentration discriminating between metallic and thermally activated conductivity is equal to about $1.6 \times 10^{18} \text{ cm}^{-3}$, which is in good agreement with theoretical considerations in Refs. 6 and 7. The electron transport measurements show that the metal-insulator transition in GaN:Si has many features characteristic of the Mott-Hubbard type of the transition. The Si donor band splits into two subbands D^0 of single- and D^- of double-occupied sites. The MIT corresponds to closing the gap between the two subbands, and at the same time the activation energy to the GaN conduction

band disappears. Beyond the MIT, the two donor subbands and the GaN conduction band overlap and lose their structure. In the next section, we will show that the two electrons at a double-occupied donor site are antiferromagnetically coupled. This will be concluded from ESR.

VI. DOUBLE-OCCUPIED STATES: CONCLUSIONS FROM ESR

Figure 7 shows the temperature dependence of the ESR amplitude in HVPE-grown GaN:Si. To obtain the amplitude of the signal, the Dysonian line shape was decomposed into an absorption and a dispersion part. The amplitude of the absorption part is plotted in Fig. 7. Corrections for the skin effect were taken into account when necessary. The resonance amplitudes show a $1/T$ dependence characteristic of the Curie paramagnetism. The single-occupied Si donor states form a classical paramagnetic band. The concentration of Si donors being in a neutral D^0 state can be calculated from Fig. 7 by comparing the amplitude of the resonance to the calibrated standard sample. The concentration of D^0 centers determined in this way is plotted in Fig. 8 versus the $n_{\text{Si}} - n_a$ parameter.

The amplitude of the ESR is proportional to the number of paramagnetic centers in a sample. Neutral donor concentrations obtained in this way for n -type GaN reported in the literature agree reasonably with the nominal doping.^{11,13} This simple rule, however, fails when approaching the MIT; see Fig. 8. Indeed, the concentration of neutral donors is proportional to $n_{\text{Si}} - n_a$ for the lightest doped sample ($3.3 \times 10^{16} \text{ cm}^{-3}$), but for the two samples close to the MIT (1.5×10^{18} and $1.6 \times 10^{18} \text{ cm}^{-3}$), the resonance amplitude

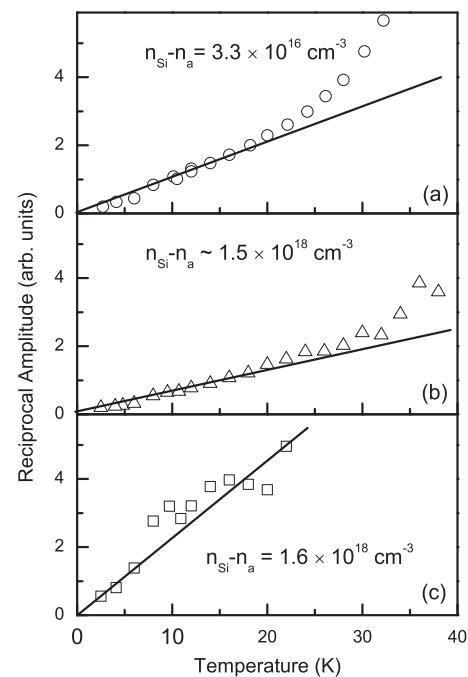


FIG. 7. Temperature dependence of ESR amplitudes for HVPE-grown GaN:Si with $n_{\text{Si}} - n_a$ equal to (a) $3.3 \times 10^{16} \text{ cm}^{-3}$, (b) $1.5 \times 10^{18} \text{ cm}^{-3}$, and (c) $1.6 \times 10^{18} \text{ cm}^{-3}$. Solid lines are guides to the eye. Linear dependence of the reciprocal amplitude on temperature indicates Curie paramagnetism.

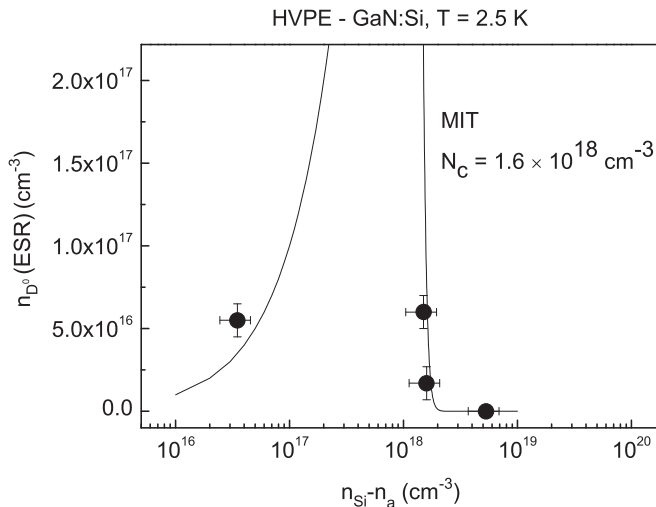


FIG. 8. Concentration of neutral Si donors determined from the amplitude of the ESR signal vs $n_{Si} - n_a$. Solid line is given by the Gibbs distribution, Eq. (2). At low Si concentrations, the amplitude of the ESR signal scales linearly with $n_{Si} - n_a$. When approaching the metal-insulator transition, a mass occupation of D^- states occurs, resulting in a rapid drop of the ESR signal amplitude.

is drastically reduced with respect to the $n_{Si} - n_a$. Finally, for the highest doped sample ($5.3 \times 10^{18} \text{ cm}^{-3}$), we did not record any ESR signal. The rapid drop of the ESR amplitude when approaching the MIT can be well explained by filling double-occupied D^- states, occurring at the expense of D^0 centers. When spins of the two electrons occupying the D^- site are antiparallel coupled, they form a nonmagnetic center that is not responsive to the ESR technique. The solid line in Fig. 8 shows the following dependence:

$$n_{D^0} = (n_{Si} - n_a) f^{(1)}, \quad (2)$$

where n_{D^0} is the concentration of neutral Si donors (which is seen by ESR), $n_{Si} - n_a$ is the difference between the total concentration of Si and the concentration of acceptors, and finally $f^{(1)}$ is the Gibbs distribution describing the probability of finding one electron on the two-electron center. The parameters necessary to calculate the probability are as follows: the position of the Fermi level and the location of the D^0 and D^- levels, which are obtained from the Hall data. When the Fermi level is located between the D^0 and D^- levels, the lower level (D^0) is fully occupied and the upper level (D^-) is practically empty. The situation changes drastically when the Fermi level approaches the upper (D^-) level. The mass occupation of the D^- level occurs, which is followed by an emptying of the D^0 level. Although the above description is only for the energy levels, not the bands, it can provide a simple quantitative understanding of the diminishing number of donors in the neutral charge state occurring at the MIT. It is worth stressing that in metallic GaN:Si samples that are beyond the MIT, the electronic states formed from Si donor bands and the GaN conduction band are double-occupied with vanishing magnetic moment.

Excitation of the donor electrons from the single-occupied D^0 band to the double-occupied D^- band influences both the resonance amplitude and the linewidth. In Fig. 7, a rapid drop

of the ESR amplitude diverging from the $1/T$ dependence is clearly visible at temperatures higher than 25 K. This indicates a loss of the D^0 electrons, which, according to the proposed model, are thermally excited to the D^- band.

The linewidth, and thus electron spin relaxation, seems to be even more influenced by the presence of the D^- band. The excitation to the D^- states shortens the electron lifetime in the D^0 band both with increasing temperature and increasing the doping concentration (Fig. 3). The electron lifetime in the D^0 band imposes an upper limit to the spin relaxation time T_2 . This is a very strong effect that is particularly dominant in samples approaching the MIT. We stress here that the ESR linewidth for samples close to the MIT provides a direct measure of the electron lifetime in the D^0 band.

It is worth noting here that we cannot unambiguously conclude what the origin of the D^- band is either from Hall effect measurements or from the ESR. The Mott-Hubbard model links the D^- band to the upper subband originating from a splitting of the donor band into single- and double-occupied states. However, one can think about another scenario, i.e., when the increased doping concentration promotes the creation of native defects introducing the double-occupied states at the bottom of the GaN conduction band. In principle, we cannot exclude such a possibility. However, it has been established that doping with donors promotes rather deep acceptor centers to compensate the donors.²⁸ This effect is visible even in our electron transport analysis, where, despite the increasing Si doping, the compensation ratio remains roughly constant. The silicon DX centers are also not likely to be responsible for the shallow double-occupied donor band, as they have been shown to form unstable configurations.²⁹ So far, the splitting of the Si donor band into single- and double-occupied states provides the most plausible explanation. This terminology has been used throughout the paper.

VII. CONCLUSIONS

A number of theoretical approaches have been developed for the metal-insulator transition.⁶ In this paper, we have shown that the real metal-insulator transition in GaN:Si shows many features characteristic of the Mott-Hubbard type of the MIT: the existence of a paramagnetic D^0 band of single-occupied donor sites (27 meV below the bottom of the GaN conduction band) and a nonmagnetic D^- band of double-occupied electronic states (2.7 meV below the bottom of the GaN conduction band). The metal-insulator transition corresponds to simultaneously closing the gap between the two subbands and a vanishing of the activation energy for electron transport in the GaN conduction band. This occurs at the critical Si concentration equal to about $n_{Si} - n_a = 1.6 \times 10^{18} \text{ cm}^{-3}$. When approaching the MIT, damping of the electronic magnetic moment occurs due to double occupation of electronic states. Finally, for metallic samples beyond the MIT, the magnetic moment vanishes.

A new spin relaxation mechanism has been observed in samples approaching the MIT. The electron spin relaxation time T_2 is constrained by the limited electron lifetime in the D^0 band, shortening both when increasing temperature and the Si concentration. It is the dominant spin relaxation mechanism at this doping level. The ESR linewidth provides

in this case a direct measure of the electron lifetime in the D^0 band. Above the metal-insulator transition, it seems that there is no need to consider the electron spin relaxation, as the conducting electrons fill double-occupied electronic states with antiparallel coupled spins.

ACKNOWLEDGMENTS

This work has been supported by funds for science, Grants No. PBZ/MNiSW/07/2006/39 and No. N N202 1058 33, Poland.

-
- ¹C. Skierbiszewski, Z. R. Wasilewski, M. Siekacz, A. Feduniewicz, P. Perlin, P. Wisniewski, J. Borysiuk, I. Grzegory, M. Leszczyński, T. Suski, and S. Porowski, *Appl. Phys. Lett.* **86**, 011114 (2005).
- ²A. P. Zhang, F. Ren, T. J. Anderson, C. R. Abernathy, R. K. Singh, P. H. Holloway, S. J. Pearton, D. Palmer, and G. E. McGuire, *Crit. Rev. Solid State Mater. Sci.* **27**, 1 (2002).
- ³B. Beschoten, E. Johnston-Halperin, D. K. Young, M. Poggio, J. E. Grimaldi, S. Keller, S. P. DenBaars, U. K. Mishra, E. L. Hu, and D. D. Awschalom, *Phys. Rev. B* **63**, 121202(R) (2001).
- ⁴J. H. Buss, J. Rudolph, F. Natali, F. Semond, and D. Hagele, *Phys. Rev. B* **81**, 155216 (2010).
- ⁵A. Wolos and M. Kaminska, in *Magnetic Impurities in Wide Band-gap III-V Semiconductors*, in *Spintronics, Semiconductors and Semimetals 82*, edited by T. Dietl, D. D. Awschalom, and M. Kaminska (Elsevier, San Diego, 2008), p. 325.
- ⁶A. Ferreira da Silva and C. Persson, *J. Appl. Phys.* **92**, 2550 (2002).
- ⁷A. Ferreira da Silva, C. Moyses Araujo, B. E. Sernelius, C. Persson, R. Ahuja, and B. Johansson, *J. Phys. Condens. Matter* **13**, 8891 (2001).
- ⁸B. I. Shklovskii and A. L. Efros, *Electronic Properties of Doped Semiconductors*, in Springer Series in Solid-State Sciences Vol. **45**, edited by M. Cardona, P. Fulde, and H.-J. Queisser (Springer-Verlag, Berlin, 1984).
- ⁹I. Grzegory, B. Lucznik, M. Bockowski, and S. Porowski, *J. Cryst. Growth* **300**, 17 (2007).
- ¹⁰I. Grzegory, B. Lucznik, M. Bockowski, B. Pastuszka, M. Krysko, G. Kamler, G. Nowak, and S. Porowski, in *Gallium Nitride Materials and Devices*, edited by C. W. Litton, J. G. Grote, H. Morkoc, A. Madhukar [*Proc. SPIE* **6121**, 612107 (2006)].
- ¹¹W. E. Carlos, J. A. Freitas Jr., M. A. Khan, D. T. Olson, and J. N. Kuznia, *Phys. Rev. B* **48**, 17878 (1993).
- ¹²M. Palczewska, B. Suchanek, R. Dwilinski, K. Pakula, A. Wagner, and M. Kaminska, *MRS Internet J. Nitride Semicond. Res.* **3**, article 45 (1998).
- ¹³E. R. Glaser *et al.*, *Mater. Sci. Eng. B* **93**, 39 (2002).
- ¹⁴F. J. Dyson, *Phys. Rev.* **98**, 349 (1955).
- ¹⁵G. Feher and A. F. Kip, *Phys. Rev.* **98**, 337 (1955).
- ¹⁶Ch. P. Poole, *Electron Spin Resonance: A Comprehensive Treatise on Experimental Techniques* (Wiley Interscience, New York, 1967).
- ¹⁷Ch. Poole and H. A. Farach, *The Theory of Magnetic Resonance* (Wiley Interscience, New York, 1972).
- ¹⁸E. Michaluk, Ph.D. thesis, Institute of Physics, Polish Academy of Sciences, 2010.
- ¹⁹A. Abragam and B. Bleaney, *Electron Paramagnetic Resonance of Transition Ions*, (Clarendon, Oxford, 1970).
- ²⁰A. Wolos, M. Piersa, G. Strzelecka, K. P. Korona, A. Hruban, and M. Kaminska, *Phys. Status Solidi C* **6**, 2769 (2009).
- ²¹Yu. A. Gurvich, A. P. Melnikov, L. N. Shestakov, and E. M. Gershenson, *Laser Phys.* **8**, 541 (1998).
- ²²E. A. Davis and W. D. Compton, *Phys. Rev.* **140**, A2183 (1965).
- ²³N. F. Mott, *Metal-Insulator Transitions* (Taylor & Francis, New York, 1990).
- ²⁴Y. J. Wang, H. K. Ng, K. Doverspike, D. K. Gaskill, T. Ikedo, I. Akasaki, and H. Amano, *J. Appl. Phys.* **79**, 8007 (1996).
- ²⁵W. Gotz, N. M. Johnson, C. Chen, H. Liu, C. Kuo, and W. Imler, *Appl. Phys. Lett.* **68**, 3144 (1996).
- ²⁶D. A. Woodbury and J. S. Blakemore, *Phys. Rev. B* **8**, 3803 (1973).
- ²⁷V. L. Bonch-Bruевич and S. G. Kalashnikov, *Fizika Poluprovodnikov (Physics of Semiconductors)* (Nauka, Moscow, 1977).
- ²⁸P. Boguslawski, E. L. Briggs, and J. Bernholc, *Phys. Rev. B* **51**, 17255 (1995).
- ²⁹P. Boguslawski and J. Bernholc, *Phys. Rev. B* **56**, 9496 (1997).